10-31-2012

Scanning Angle Plasmon Waveguide Resonance Raman Spectroscopy for the Analysis of Thin Polystyrene Films

Matthew W. Meyer
Iowa State University

Kristopher J. McKee
Iowa State University

Vy H.T. Nguyen
Iowa State University

Emily A. Smith
Iowa State University, esmith1@iastate.edu

Scanning Angle Plasmon Waveguide Resonance Raman Spectroscopy for the Analysis of Thin Polystyrene Films

Abstract

Scanning angle (SA) Raman spectroscopy was used to characterize thin polymer films at a sapphire/50 nm gold film/polystyrene/air interface. When the polymer thickness is greater than ~260 nm, this interface behaves as a plasmon waveguide; Raman scatter is greatly enhanced with both p- and s-polarized excitation compared to an interface without the gold film. In this study, the reflected light intensities from the interface and Raman spectra were collected as a function of incident angle for three samples with different polystyrene thicknesses. The Raman peak areas were well modeled with the calculated mean-square electric field (MSEF) integrated over the polymer film at varying incident angles. A 412 nm polystyrene plasmon waveguide generated 3.34× the Raman signal at 40.52° (the plasmon waveguide resonance angle) compared to the signal measured at 70.4° (the surface plasmon resonance angle). None of the studied polystyrene plasmon waveguides produced detectable Raman scatter using a 180° backscatter collection geometry, demonstrating the sensitivity of the SA Raman technique. The data highlight the ability to measure polymer thickness, chemical content, and, when combined with calculations of MSEF as a function of distance from the interface, details of polymer structure and order. The SA Raman spectroscopy thickness measurements agreed with those obtained from optical interferometery with an average difference of 2.6%. This technique has the potential to impact the rapidly developing technologies utilizing metal/polymer films for energy storage and electronic devices.

Disciplines

Chemistry | Materials Chemistry | Organic Chemistry | Other Chemistry | Physical Chemistry

Comments

Reprinted (adapted) with permission from *The Journal of Physical Chemistry C,* 116(47); 24987-24992. Doi: 10.1021/jp308882w.

THE JOURNAL OF PHYSICAL CHEMISTRY C

Article

pubs.acs.org/JPCC

Scanning Angle Plasmon Waveguide Resonance Raman Spectroscopy for the Analysis of Thin Polystyrene Films

Matthew W. Meyer,[†,‡] Kristopher J. McKee,[†,‡] Vy H. T. Nguyen,[†,‡] and Emily A. Smith*[,†,‡]

[†]Ames Laboratory, U.S. Department of Energy, Ames, Iowa 50011-3111, United States

[‡]Department of Chemistry, Iowa State University, Ames, Iowa 50011-3111, United States

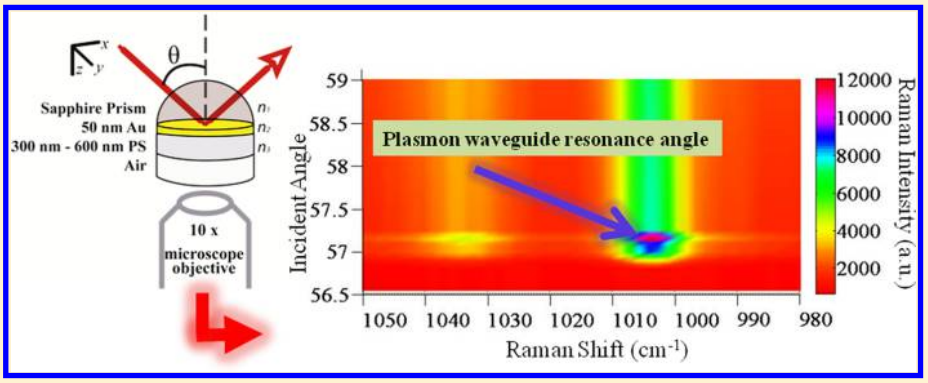

ABSTRACT: Scanning angle (SA) Raman spectroscopy was used to characterize thin polymer films at a sapphire/50 nm gold film/polystyrene/air interface. When the polymer thickness is greater than ~260 nm, this interface behaves as a plasmon waveguide; Raman scatter is greatly enhanced with both p- and s-polarized excitation compared to an interface without the gold film. In this study, the reflected light intensities from the interface and Raman spectra were collected as a function of incident angle for three samples with different polystyrene thicknesses. The Raman peak areas were well modeled with the calculated mean-square electric field (MSEF) integrated over the polymer film at varying incident angles. A 412 nm polystyrene plasmon waveguide generated 3.34× the Raman signal at 40.52° (the plasmon waveguide resonance angle) compared to the signal measured at 70.4° (the surface plasmon resonance angle). None of the studied polystyrene plasmon waveguides produced detectable Raman scatter using a 180° backscatter collection geometry, demonstrating the sensitivity of the SA Raman technique. The data highlight the ability to measure polymer thickness, chemical content, and, when combined with calculations of MSEF as a function of distance from the interface, details of polymer structure and order. The SA Raman spectroscopy thickness measurements agreed with those obtained from optical interferometery with an average difference of 2.6%. This technique has the potential to impact the rapidly developing technologies utilizing metal/polymer films for energy storage and electronic devices.

INTRODUCTION

Total internal reflection (TIR) Raman spectroscopy is an analytical technique used to measure chemical content near an interface.[1−3] In a typical TIR Raman experiment the illuminating light is directed onto a prism/sample/bulk interface at a precise incident angle.[4] At angles above the critical angle, total internal reflection conditions occur, and a surface-sensitive evanescent wave is generated in the sample. TIR-Raman spectroscopy has been useful in studying films, surfactants, plants, and adsorbates at various interfaces.[5−8] As with conventional Raman spectroscopy, TIR Raman spectroscopy has the benefits of being noninvasive, fast, and requiring minimal sample preparation provided the sample can be optically coupled to the prism. For conditions where the same amount of analyte is probed, the TIR Raman geometry acts as a signal enhancement mechanism, and excellent signal-to-noise ratio spectra are possible for thin films using several second acquisition times.

TIR-Raman spectroscopy has been combined with surface plasmon resonance (SPR-Raman spectroscopy) using thin noble metal films to provide predictable signal enhancements, high experimental reproducibility, and the ability to accurately model data with theoretical calculations.[9−11] An example interface used for SPR-Raman spectroscopy is prism/gold/sample/bulk medium. The SPR phenomenon occurs at incident angles where propagating surface-plasmon-polaritons are excited in the metal film. Under these conditions, the generated evanescent wave extends spatially into the sample. This field can produce Raman scatter from the molecules located within $D_p/2$, where D_p is the penetration depth of the evanescent wave.[4] McKee et al. used SPR-Raman spectroscopy for reproducible Raman enhancements ranging from 4.7× to

Received: September 6, 2012
Revised: October 24, 2012
Published: October 31, 2012

dx.doi.org/10.1021/jp308882w | J. Phys. Chem. C 2012, 116, 24987−24992

3.7× for aqueous pyridine and nitrobenzene at a sapphire/gold/sample interface compared to a sapphire/sample interface.[12] The latter signal is already approximately an order of magnitude greater than probing the same amount of analyte using normal illumination geometries. The enhancements from the smooth gold films allowed for the detection of single monolayers of benzenethiol and 4-mercaptopyridine with nonresonant excitation.

Thin polymer films are critical components of many devices including sensors, coatings, and medical implants.[13] Common optical methods for measuring thin polymer films include ellipsometry, optical interferometry, attenuated total internal reflection infrared spectroscopy, and TIR-Raman spectroscopy.[14−16] TIR-Raman spectroscopy provides the advantage of measuring thickness, structure, and chemical content simultaneously, at a variety of interfaces.[17−19] TIR-Raman spectroscopy was used to study thin polymer films at a glass interface.[20,21] Most recently, Kivioja et al. used TIR-Raman spectroscopy at a fixed incident angle to measure thin polystyrene films on a sapphire interface.[22]

Optical waveguides can be used to confine incident light within a sample or carry incident light to the sample for the analysis of thin films.[23] When a polymer film of approximately $\lambda/2\eta$ (λ wavelength of excitation, η index of refraction of the sample) thickness is coated on a surface plasmon supporting metal film with a bulk air layer, the polymer can act as a radiative or "leaky" waveguide.[24,25] Recently, leaky waveguides have been used as biosensors for clinical diagnosis and bacterial analysis.[24,26] Kanger et al. used waveguides in Raman spectroscopy experiments to measure the orientation of porphyrin monolayers.[27] Their results showed the preferred orientation of the molecules can be obtained using deviations of the monolayer's depolarization ratios from those measured in the bulk. Zimba et al. calculated the expected effects of excitation wavelength on waveguide Raman spectra at a quartz/polymer interface.[28]

At the plasmon waveguide interface, large increases in the interfacial mean square electric field relative to the incident field (MSEF) are generated at incident angles where plasmon waveguide resonances (PWR) are excited.[29] Until recently, a majority of PWR spectroscopy measurements only utilized the reflected light intensity from the interface.[30] At the PWR angles, a sharp attenuation of the reflected light occurs with both p- and s-polarized incident light. When PWR and Raman spectroscopies are combined (PWR Raman spectroscopy), strong enhancements of the Raman signal are expected at the PWR angle(s) due to enhancements in the MSEF. The incident angle(s) where plasmon waveguide resonances are excited depends on the thickness of the polymer layer; thus, polymer films of different thickness should generate unique patterns of Raman scattering intensities as the incident angle is scanned. One advantage of PWR Raman spectroscopy, compared to SPR Raman spectroscopy is that both p-polarized light (electric field oriented parallel to the plane of incidence) and s-polarized (perpendicular) light can be used to produce MSEF in the X, Y, and Z direction ($MSEF_X$, $MSEF_Y$, $MSEF_Z$), where X and Y extend in the focal plane and Z is perpendicular to the focal plane. In SPR-Raman spectroscopy no $MSEF_Y$ component is generated.

The goals of this study are to record and model the PWR Raman intensity as the incident angle of light is scanned for thin polystyrene films coated on sapphire/gold substrates. PWR-Raman measurements of polystyrene films with thicknesses of 276, 412, and 595 nm on 50 nm gold films were measured. Large Raman signals were recorded for thin polystyrene films down to a few hundred nanometers using p- and s-polarized excitation; the Raman signal and polystyrene thickness can be well modeled by electric field calculations.

EXPERIMENTAL SECTION

Sample Preparation. Gold films were prepared on 25.4 mm diameter sapphire discs (Meller Optics, Providence, RI) by deposition of 2 nm Ti followed by 49 ± 1 nm of gold at GWC Technologies Inc., Madison, WI. Prior to coating, the gold film was cleaned in ethanol and dried with a stream of N_2 gas. A 4.6, 6, or 8% (w/v) polystyrene (Sigma-Aldrich, St. Louis, MO) solution was prepared in toluene (Fisher Scientific, Waltham, MA), and 200 μL of the polystyrene solution was spin-coated on the gold-coated sapphire disk at 3000 rpm for 1 min using a KW-4A spin-coater (Chemat Technology, Inc. Northridge, CA). The sample was dried overnight at room temperature to make certain the solvent was completely evaporated. Gold and polymer film thicknesses were measured using a F20 series film measurement system in transmission mode (Filmetrics, San Diego, CA).

Raman Measurements. A scanning angle Raman microscope with 0.05° incident angle resolution was used to simultaneously collect Raman and reflectivity spectra.[4] Raman data were collected with angle increments ranging from 0.05° near the PWR angle to 0.20° far away from the PWR angle. Incident excitation was from a 785 nm laser with 210 mW measured at the sample. The laser power had a 0.4% relative uncertainty for all Raman measurements, which means the laser power varied by no more than ∼1 mW from sample to sample. A 25.4 mm diameter sapphire prism was used for the total internal reflection element, and a 10× magnification objective (Nikon, numerical aperture 0.3) was used to collect the Raman scatter. Immersion oil (Cargille Laboratories, Cedar Groove, NJ, n = 1.7800) was used to ensure optical contact between the prism and substrate. A half-wave plate in the excitation path was used to control the polarization of the incident light at the sample interface. The polarization at the sample was 99+% pure. All spectra were acquired with 1 min acquisitions, and three replicate measurements were obtained for each sample by taking consecutive scans through the entire incident angle range.

Depolarization Ratio Measurements. 20% (w/v) polystyrene was dissolved in carbon tetrachloride (Sigma-Aldrich, St. Louis, MO). A near-infrared polarizer was placed in the illumination path, and a second polarizer was placed between the microscope and spectrometer. A scrambler was added between the second polarizer and spectrometer. Raman spectra were collected for 30 s with the collection polarizer set to collect TE or TM polarized Raman scatter.

Data Analysis. All data analysis was performed using the software IGOR Pro 6.1. Raman peak areas were measured by fitting them to Gaussian curves with the "Multipeak fitting 2" algorithm. Signal-to-noise ratios (S/N) were calculated as the maximum of the 1001 cm^{-1} peak intensity after background subtraction divided by the standard deviation of the noise measured from 920 to 950 cm^{-1} in a region of the spectrum where no analyte peaks were present. Fresnel calculations were used to model the reflected light intensity.[31] The Fresnel calculations account for the 0.5° incident angle spread that results from focusing within the prism.

Mean-Square Electric Field Calculations. 3-D finite-difference-time-domain (FDTD)-based simulations were used to calculate the MSEF at varying incident angles (EM Explorer, San Francisco, CA). A Yee cell size of 5 nm was used for all FDTD simulations, and the calculations account for multiple reflections within the polymer layer. The interface had a sapphire prism (η_o 1.761, η_e 1.753), 50 nm gold film (η 0.143 + 4.799i), and a polystyrene layer of varying thickness (η 1.578), and the bulk medium was air.[32,33] The angular resolution used for the calculations was 0.05° near the PWR angle and 0.5° elsewhere.

RESULTS AND DISCUSSION

Calculated Reflectivity and Predicted Raman Peak Areas for a Sapphire/50 nm Au/Polystyrene/Air Interface. The purpose of this study is to measure and model the PWR Raman signal for polystyrene waveguides of varying thickness. Determining the polymer thickness and chemical composition is possible by analyzing the PWR-Raman spectra as a function of incident angle. Figure 1 shows the calculated reflected light intensity (Figure 1A,C) and MSEF integrated over the polymer thickness (Figure 1B,D) at a sapphire/50 nm gold film interface containing a 276 nm (solid black), 412 nm (solid gray), or 595 nm (dotted black) polystyrene film. Using p-polarized excitation, $MSEF_{Z+X}$ is generated (Figure 1B), while s-polarized excitation generates $MSEF_Y$ (Figure 1D). The coordinate system used in this work is shown in Figure 1.

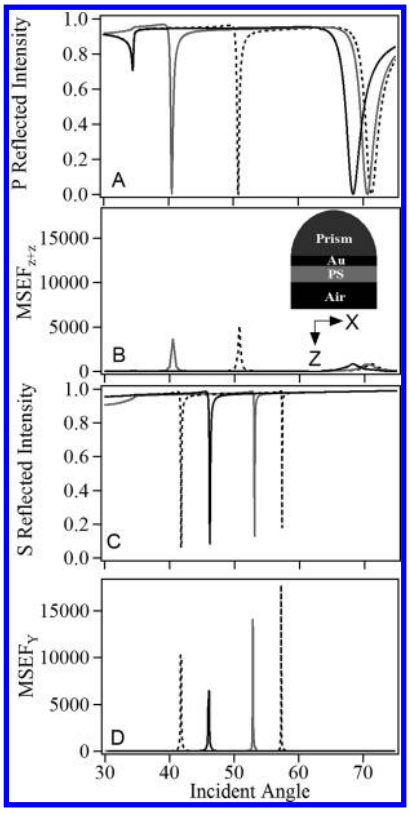

Figure 1. Calculated reflectivity (A and C) and mean-square electric field integrated over the polymer stack (MSEF, B and D) for a sapphire prism/50 nm gold/polystyrene (PS)/air interface. The thickness of the polystyrene film is 276 nm (solid black), 412 nm (solid gray), or 595 nm (dotted black). The reflectivity calculations used a 0.5° incident angle spread in the excitation light. The p-polarized incident light (A, B) generates a MSEF in the *Z* and *X* directions, and s-polarized incident light (C, D) generates a MSEF in the *Y* direction. The inset schematic shows the coordinate system used in this work; the *Y*-axis points toward the reader.

For p-polarized excitation, the reflected light intensity is attenuated at some angles within the angle range of 34.5°−60° for all three interfaces. In this range, the angle where the attenuation of the reflected light intensity occurs is commonly referred to at the PWR angle.[34] The PWR angle undergoes a shift from 34.51° to 40.52° when the film thickness is increased from 276 to 412 nm. The reflectivity curve for the 595 nm polystyrene film contains two waveguiding modes (m = 0 and m = 1) using p-polarized excitation, giving rise to PWR angles of 34.48° and 50.77°, respectively. The PWR angle generated with s-polarized light is not the same as the PWR angle generated with p-polarized light. Although the associated angles and magnitudes are different, qualitatively, the same trends are expected in the reflectivity curves using s-polarized excitation. The shift in the PWR angle is sensitive to small changes in the polystyrene thickness. For example, the PWR angle for a 600 nm polystyrene film will undergo a 0.37° (p-polarization) and a 0.15° (s-polarization) shift when the thickness is increased to 610 nm.

For polystyrene films and using a 785 nm wavelength laser, the cutoff thickness for PWR Raman spectroscopy using a prism/gold/polystyrene/air interface with p- and s-polarized excitation is approximately 260 and 140 nm, respectively. For films thinner than this, PWR Raman spectroscopy using a prism/gold/silica/polystyrene/bulk medium interface may be utilized.[35] In theory polystyrene films of several micrometers can be measured with PWR Raman spectroscopy. A 5 μm film will produce 15 distinct waveguide modes with p- or s-polarized excitation over an angle range of 35°−65°. In practice, films of several micrometers thickness present an experimental challenge due to the required angular resolution. The fwhm for the PWR peaks corresponding to polymer thickness below ~600 nm range from 0.04° to 0.5°; the PWR peaks with s-polarized excitation are generally narrower than those with p-polarized excitation. Experimental measurements should have an angular resolution equal to or smaller than the fwhm.

The sharp attenuation of the reflected light at the PWR angle is a near mirror reflection of the corresponding MSEF curves (Figure 1B,D), which is expected to model the Raman scatter. The 276 nm polystyrene film is at the cusp of the polymer thickness required to generate a PWR peak using p-polarized incident light and is associated with the lowest calculated MSEF (maximum integrated $MSEF_{Z+X}$ 38.1). The 412 and 595 nm polystyrene films, on the other hand, exhibit distinct PWR peaks. In contrast to p-polarized excitation, even the thinnest film is expected to exhibit significant Raman signals (maximum integrated $MSEF_Y$ up to 17700) using s-polarized excitation.

At an angle greater than 60° there is a broad attenuation dip in the reflectivity curve using p-polarized excitation. The angle where this dip occurs is referred to as the SPR angle and is the angle where the maximum Raman scatter is predicted in SPR-Raman spectroscopy. The MSEF enhancement is similar at the SPR angle regardless of whether the interface supports waveguide modes (Table 1). On the other hand, the MSEF enhancement is greater at the PWR angle than the SPR angle, and s-polarized light generates a $MSEF_Y$ component at the waveguide interface.

Compared to an interface without the gold film, the calculated MSEF at the gold film is approximately 10−50× higher. Since the MSEF is proportional to the expected Raman

dx.doi.org/10.1021/jp308882w | J. Phys. Chem. C 2012, 116, 24987−24992

Table 1. Comparison of Surface Plasmon Resonance and Plasmon Waveguide Resonance Parameters for Thin Polystyrene Films at the Sapphire/50 nm Gold/Polystyrene Interface

polymer thickness and platform	SPR/PWR angle (deg)	fwhm (deg)	$MSEF_{Ex+Ez}$ integrated over polymer film	$MSEF_{Ey}$ integrated over polymer film
non-waveguide (100 nm)				
SPR (p)	50.69	2.24	786	0.0
waveguide (412 nm)				
SPR (p)	70.67	2.76	839	0.0
PWR (p)	40.52	0.48	3776	0.0
PWR (s)	52.95	0.12	0.0	14060

scatter generated at the interface, it is proposed that the PWR Raman measurements will generate more Raman scatter when the same polymer thickness is considered. The expected, large PWR Raman signal means one or several second acquisition times should generate significant Raman scatter, which decreases the total analysis time per sample without compromising the spectral signal-to-noise ratio.

Experimental Reflectivity Curves and Determination of Polystyrene Thickness. Reflectivity curves collected with p-polarized incident light are shown in Figure 2A, B, C for three thicknesses of polystyrene. Only the films fabricated using 6 or 8% (w/v) polystyrene generated a PWR peak, while the 4.6% (w/v) film produced only an SPR peak. The reflectivity curve of a 8% (w/v) polystyrene film using s-polarized incident light is shown in Figure 2D. The polystyrene film thickness was determined by modeling the location of the PWR or SPR angle(s) using Fresnel calculations.[31] While holding all other parameter constant, the thickness of the polystyrene layer was varied until the best fit was obtained (Figure 2: A, 276 nm; B, 412 nm; and C, D, 595 nm). For the 595 nm polystyrene film, the thickness that generated the best fit to the PWR peaks did not fit the SPR peak as well. A small increase in the imaginary component of gold's index of refraction will shift the calculated SPR peak to the left, with minimal perturbations to the PWR peak. This suggests there is heterogeneity in the gold films on which the polymer was deposited, which is reasonable since they were fabricated in several batches. For the 595 nm polystyrene film using s-polarized excitation, the attenuation of the reflected light corresponding to the $m = 1$ guided mode at 41.80° is experimentally measured, but the predicted $m = 0$ mode at 57.57° is not. The fwhm of the PWR reflectivity peaks are calculated to be roughly 6× narrower than the SPR peaks. The lack of a measured PWR peak at 57.57° is attributed to the narrowness of the PWR peak (fwhm 0.04°) and the instrument's angular resolution of 0.05°. This is also the reason the experimental reflectivity minima is less than predicted in several instances.

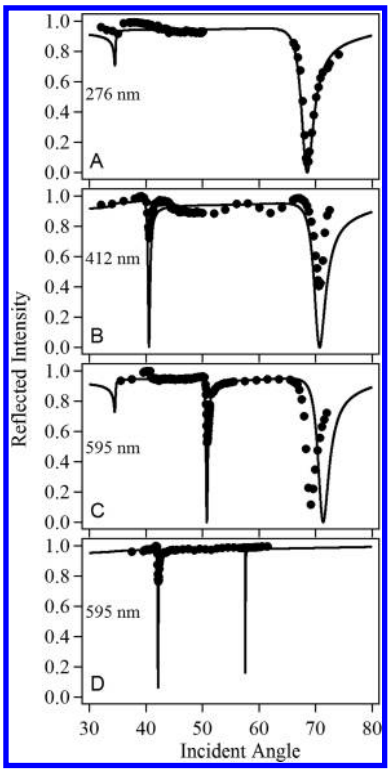

Figure 2. Reflectivity spectra (solid symbols) from a sapphire prism/50 nm gold/polystyrene (PS)/air interface: (A) 276 nm PS; (B) 412 nm PS; (C) 595 nm PS collected with p-polarized incident excitation. (D) Sapphire prism/50 nm gold/595 nm polystyrene (PS)/air interface collected with s-polarized incident excitation. The solid lines are calculated reflectivities for the same interfaces.

The polymer thicknesses obtained from the modeled reflectivity data agree with a calibration curve generated using optical interferometry (data not shown). The difference between the scanning angle Raman and optical interferometry measurements is associated with an average difference of 2.6% for all three films. Potential errors involved in the thickness measurement include the instrument's incident angle calibration, the finite angular resolution of the instrument, and uncertainties in the gold film thickness or indices of refraction of any of the interfacial layers.

PWR-Raman Spectra of Polystyrene Films. Raman spectra are shown in Figure 3 for the same samples used to simultaneously generate the reflectivity data in Figure 2. Assignments for the most intense peaks are shown in Table 2. The Raman spectra were collected at an incident angle of 68.40° (p, 276 nm polystyrene), 40.52° (p, 412 nm polystyrene), 50.77° (p, 595 nm polystyrene), or 41.80° (s, 595 nm polystyrene), which correspond to the incident angles that generated the greatest Raman scatter. For the 276 nm film, the highest Raman scatter was collected at the SPR angle, which is expected since no PWR peak was measured for this film. The higher 1003 cm^{-1} peak intensity for s-polarized excitation compared to p-polarized excitation quantitatively agrees with the calculated MSEF from Figure 1 when the magnitude of the reflected light intensity is considered.

The PWR Raman spectrum's S/N ratio for the 412 nm polystyrene film is 602 (Figure 3B) using a 60 s acquisition time, which is significantly better than the S/N ratio of 28 for a 580 nm film at the sapphire interface without a gold film (data not shown). The gold film enables the acquisition time to be reduced to a couple of seconds per spectrum to achieve the same S/N ratio as a 60 s acquisition for a similar film thickness deposited on sapphire. It should also be stated that none of the polystyrene waveguides produced detectable Raman scatter using a 180° backscatter geometry with the same instrument.

The insets in Figure 3C,D show the spectra normalized to the most intense polystyrene peak (1003 cm^{-1}) to compare the relative peak intensities using different excitation polarizations. PWR-Raman measurements of polystyrene show certain bands

dx.doi.org/10.1021/jp308882w | J. Phys. Chem. C 2012, 116, 24987−24992

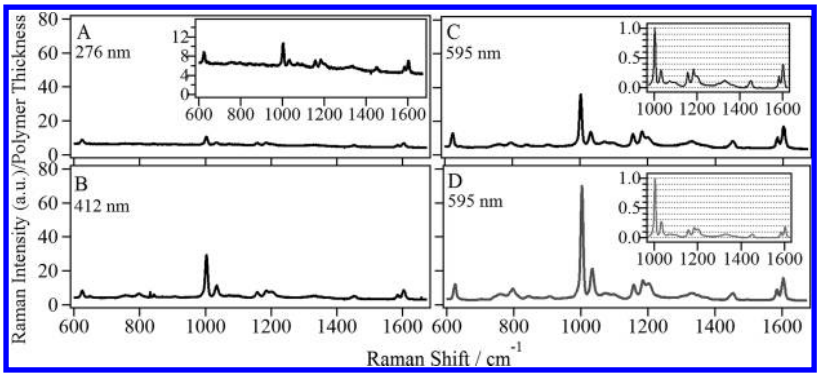

Figure 3. Raman spectra of a sapphire prism/50 nm gold/polystyrene (PS)/air interface: (A) 276 nm PS; (B) 412 nm PS; (C) 595 nm PS collected with p-polarized incident excitation at 68.40°, 40.52°, and 50.77° incident angle, respectively. (D) Sapphire prism/50 nm gold/595 nm polystyrene (PS)/air interface collected with s-polarized incident excitation at 41.80° incident angle. The inset in (A) shows the same spectrum at a smaller scale. The inset in (C) and (D) show the normalized spectra so that relative peak intensities can be compared. All spectra have been divided by their respective film thickness to emphasize differences in the scattering intensity due to differences in the MSEF. The slight elongation of the beam size at larger incident angles (e.g., 242 μm × 179 μm at 40° and 271 μm × 177 μm at 68°) has not been accounted for in the spectra.

Table 2. Peak Location, Assignment and Relative Intensity Ratio for s/p-Polarized Excitation for PWR Raman Spectra of Polystyrene; Measured Depolarization Ratios for a Solution of Polystyrene

peak (cm^{-1})	assignment (Wilson notation)[37,38]	rel int (S)/(P): PWR Raman spectroscopy	solution depolarization ratio: normal illumination Raman spectroscopy
624	ν_{6b}	0.5	1.08
760		0.8	ca. 0
795	ν_{11}	1	ca. 0
843	$\nu_{10a/17b}$	0.5	
906	vinyl	0.5	
1003	ν_{1}	1	0.06
1031	ν_{18a}	0.9	ca. 0
1073		0.5	
1097		0.6	
1156	ν_{9b}	0.5	0.84
1184	ν_{9a}	0.5	0.65
1201	ν_{7a}	0.8	ca. 0
1304	vinyl	0.6	
1330	ν_{14}	0.5	
1346	ν_{3}	0.5	
1368	vinyl	0.5	
1451	$\nu_{19b/a}$	0.5	
1584	ν_{8b}	0.5	1.22
1602	ν_{8a}	0.5	0.91

produce more Raman scatter with p-polarized excitation compared to s-polarized excitation when the spectra are normalized to the 1003 cm^{-1} polarized peak. Table 2 lists the ratio of the PWR Raman peak intensity for s/p-polarized excitation and the 595 nm film. Also shown in Table 2 are the depolarization ratios measured for a solution of polystyrene with the 180° backscattering geometry. The polarized bands produced a s/p-peak intensity ratio greater than 0.8 when comparing spectra normalized to the 1003 cm^{-1} peak. The depolarized bands produce ratios from 0.5 to 0.6. The origin for the differences in the scanning angle Raman spectra using orthogonal excitation has been previously discussed.[12]

Measured Raman Peak Areas and Calculated MSEF. The Raman peak areas of the polystyrene 1003 cm^{-1} band are plotted as a function of incident angle in Figure 4 for the same samples discussed above. The Raman peak areas fit to the

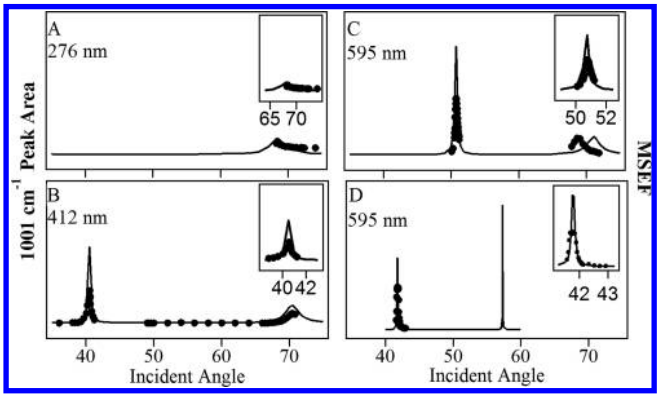

Figure 4. Raman 1003 cm^{-1} peak areas (black spheres) as a function of incident angle for a sapphire prism/50 nm gold/polystyrene (PS)/air interface: (A) 276 nm PS; (B) 412 nm PS; (C) 595 nm PS collected with p-polarized incident excitation. (D) Sapphire prism/50 nm gold/595 nm polystyrene (PS)/air interface collected with s-polarized incident excitation. The solid black line is the calculated MSEF (A, B, C: $MSEF_{Z+X}$; D: $MSEF_{Y}$) integrated over the entire polymer thickness. The peak area and MSEF scales are the same in (A, B, C) and are expanded 3× in (D). Example MSEF plots at select incident angles are plotted in Figure 5.

calculated integrated MSEF using the appropriate polymer thickness. The maximum Raman peak area always corresponds to the angle producing the greatest attenuation of the reflected light intensity; thus, the reflected light intensity can be used to identify the angle producing the largest Raman signal. As expected, this is in good agreement with previous SPR studies that have demonstrated that reflectivity data can be used to predict the collected Raman intensity.[12] The slight differences in the predicted Raman peak area and the measured Raman peak area can be attributed to the same causes discussed above for differences in the reflectivity data (i.e., angle resolution, angle spread, etc.).

The plot of the MSEF as a function of distance from the gold/polystyrene interface (Figure 5) at the PWR angle indicates the collected Raman scatter is not always uniformly generated throughout the polymer film. The radiative or "leaky" waveguide mode maxima are the result of interference between counterpropagating reflections.[36] For thinner polystyrene films and p-polarized excitation only a single leaky mode exists, but for all films with s-polarization and the 595 nm polystyrene film

dx.doi.org/10.1021/jp308882w | J. Phys. Chem. C 2012, 116, 24987−24992

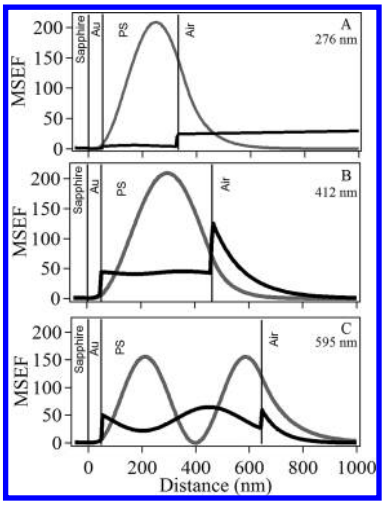

Figure 5. Calculated MSEF as a function of the distance from the interface for p-polarized (black) and s-polarized (gray) incident excitation and a sapphire prism/50 nm gold/polystyrene (PS)/air stack: (A) 276 nm PS at 34.51° (p-polarized excitation, $MSEF_{Z+X}$) and 46.20° (s-polarized excitation, $MSEF_Y$); (B) 412 nm PS at 40.52° (p) and 53.07° (s); (C) 595 nm PS at 50.77° (p) and 41.80° (s). The location of each phase in the stack is shown with a solid vertical line.

with p-polarized excitation two leaky waveguide modes exist. Both the polymer thickness and the excitation polarization will affect the spatial distribution of the Raman signal within the polymer film. For the 276 and 412 nm polystyrene film, p-polarized excitation will produce Raman intensities nearly uniformly from the entire polymer film at the PWR angle. With thicker films using p-polarized excitation and all thicknesses using s-polarized excitation, the spatial distribution of the MSEF is more complex. For example, the strongest Raman intensity will be generated near the center of the polymer films using s-polarized excitation with the 412 nm film at the PWR angle indicated in the figure legend. For films that contain more than one polymer, the MSEF versus distance plots can be used to aid in the interpretation of polymer structure or order.

CONCLUSIONS

This proof of principle study shows scanning angle plasmon waveguide resonance Raman spectroscopy can measure thin polymer films with predicable signal enhancements, to obtain simultaneous chemical content and accurate polymer film thicknesses. A polystyrene/air interface was used in this study to ensure that the entire Raman signal was generated from polystyrene and no polymer swelling or contamination occurred. However, other polymer films that are of high optical quality, transparent, and meet the thickness requirements of an optical waveguide could be measured, as could water or organic interfaces. Overall, the method demonstrates that PWR-Raman spectroscopy utilizing a simple plasmonic supporting system allows for optimal experimental modeling of thin films.

AUTHOR INFORMATION

Corresponding Author

*E-mail esmith1@iastate.edu.

Notes

The authors declare no competing financial interest.

ACKNOWLEDGMENTS

This research is supported by the U.S. Department of Energy, Office of Basic Energy Sciences, Division of Chemical Sciences, Geosciences, and Biosciences through the Ames Laboratory. The Ames Laboratory is operated for the U.S. Department of Energy by Iowa State University under Contract DE-AC02-07CH11358. The authors thank the Iowa State University Microelectronics Research Center for use of their Filmetrics instrument.

REFERENCES

(1) Ikeshoji, T.; Ono, Y.; Mizuno, T. *Appl. Opt.* **1973**, *12*, 2236.
(2) Woods, D. A.; Bain, C. D. *Analyst* **2012**, *137*, 35.
(3) Tisinger, L. G.; Sommer, A. J. *Microsc. Microanal.* **2004**, *10*, 1318.
(4) McKee, K. J.; Smith, E. A. *Rev. Sci. Instrum.* **2010**, *81*, 043106/1.
(5) Hoelzer, W.; Schroeter, O.; Richter, A. *J. Mol. Struct.* **1990**, *217*, 253.
(6) Woods, D. A.; Petkov, J.; Bain, C. D. *J. Phys. Chem. B* **2011**, *115*, 7341.
(7) Woods, D. A.; Petkov, J.; Bain, C. D. *J. Phys. Chem. B* **2011**, *115*, 7353.
(8) Greene, P. R.; Bain, C. D. *Colloids Surf., B* **2005**, *45*, 174.
(9) Bolduc, O. R.; Masson, J. F. *Anal. Chem.* **2011**, *83*, 8057.
(10) Liu, Y.; Xu, S. P.; Xuan, X. Y.; Zhao, B.; Xu, W. Q. *J. Phys. Chem. Lett.* **2011**, *2*, 2218.
(11) Corn, R. M.; Philpott, M. R. *J. Chem. Phys.* **1984**, *80*, 5245.
(12) McKee, K. J.; Meyer, M. W.; Smith, E. A. *Anal. Chem.* **2012**, *84*, 4300.
(13) Harsanyi, G. *Sens. Rev.* **2000**, *20*, 98.
(14) Fina, L. J. *Appl. Spectrosc. Rev.* **1994**, *29*, 309.
(15) Yang, P.; Meng, X. F.; Zhang, Z. Y.; Jing, B. X.; Yuan, J.; Yang, W. T. *Anal. Chem.* **2005**, *77*, 1068.
(16) Bohn, P. W. *Annu. Rev. Mater. Sci.* **1997**, *27*, 469.
(17) Ishizaki, F.; Kim, M. *Jpn. J. Appl. Phys.* **2008**, *47*, 1621.
(18) Fontaine, N. H.; Furtak, T. E. *Phys. Rev. B* **1998**, *57*, 3807.
(19) Zimba, C. G.; Hallmark, V. M.; Turrell, S.; Swalen, J. D.; Rabolt, J. F. *J. Phys. Chem.* **1990**, *94*, 939.
(20) Fontaine, N. H.; Furtak, T. E. *J. Opt. Soc. Am. B* **1997**, *14*, 3342.
(21) Ives, J. T.; Reichert, W. M. *J. Appl. Polym. Sci.* **1988**, *36*, 429.
(22) Kivioja, A. O.; Jaaskelainen, A. S.; Ahtee, V.; Vuorinen, T. *Vib. Spectrosc.* **2012**, *61*, 1.
(23) Chabay, I. *Anal. Chem.* **1982**, *54*, A071.
(24) Im, W. J.; Kim, B. B.; Byun, J. Y.; Kim, H. M.; Kim, M.-G.; Shin, Y.-B. *Sens. Actuators, B* **2012**, *173*, 288.
(25) Abbas, A.; Linman, M. J.; Cheng, Q. *Sens. Actuators, B* **2011**, *156*, 169.
(26) Zourob, M.; Mohr, S.; Brown, B. J. T.; Fielden, P. R.; McDonnell, M. B.; Goddard, N. J. *Anal. Chem.* **2005**, *77*, 232.
(27) Kanger, J. S.; Otto, C. *Appl. Spectrosc.* **2003**, *57*, 1487.
(28) Zimba, C. G.; Rabolt, J. F. *Thin Solid Films* **1991**, *206*, 388.
(29) Bradshaw, J. T.; Mendes, S. B.; Saavedra, S. S. *Anal. Chem.* **2005**, *77*, 28a.
(30) Hruby, V. J.; Alves, I.; Cowell, S.; Salamon, Z.; Tollin, G. *Life Sci.* **2010**, *86*, 569.
(31) Corn, R. M.; http://corninfor.ps.uci.edu/calculations.html.
(32) Kasarova, S. N.; Sultanova, N. G.; Ivanov, C. D.; Nikolov, I. D. *Opt. Mater.* **2007**, *29*, 1481.
(33) Bass, M.; DeCusatis, C.; Enoch, J. M.; Lakshminarayanan, V.; Li, G.; MacDonald, C.; Mahajan, V. N.; Van Stryland, E. *Handbook of Optics*, 3rd ed.; McGraw-Hill: New York, 2009; Vol. *IV*.
(34) Salamon, Z.; Tollin, G. *Spectrosc.: Int. J.* **2001**, *15*, 161.
(35) McKee, K. J.; Meyer, M. W.; Smith, E. A. *Anal. Chem.* **2012**, *84*, 9049.
(36) Zia, R.; Selker, M. D.; Brongersma, M. L. *Phys. Rev. B* **2005**, *71*, 165431.
(37) Loader, E. J. *J. Catal.* **1971**, *22*, 41.
(38) Palm, A. *J. Phys. Chem.* **1951**, *55*, 1320.